HYDROLOGICAL PROCESSES
Hydrol. Process. (2015)
Published online in Wiley Online Library
(wileyonlinelibrary.com) DOI: 10.1002/hyp.10526

The relative contributions of alpine and subalpine ecosystems to the water balance of a mountainous, headwater catchment

John F. Knowles,[1,2]* Adrian A. Harpold,[2,4,†] Rory Cowie,[1,2] Morgan Zeliff,[1,2] Holly R. Barnard,[1,2] Sean P. Burns,[1,3] Peter D. Blanken,[1] Jennifer F. Morse[2] and Mark W. Williams[1,2]

[1] *Department of Geography, University of Colorado, Boulder, CO, 80309, USA*
[2] *Institute of Arctic and Alpine Research, University of Colorado, Boulder, CO, 80309, USA*
[3] *National Center for Atmospheric Research, Boulder, CO 80307, USA*
[4] *Department of Natural Resources and Environmental Science, University of Nevada, Reno, NV, 89557, USA*

Abstract:

Climate change is affecting the hydrology of high-elevation mountain ecosystems, with implications for ecosystem functioning and water availability to downstream populations. We directly and continuously measured precipitation and evapotranspiration (*ET*) from both subalpine forest and alpine tundra portions of a single catchment, as well as discharge fluxes at the catchment outlet, to quantify the water balance of a mountainous, headwater catchment in Colorado, USA. Between 2008 and 2012, the water balance closure averaged 90% annually, and the catchment *ET* was the largest water output at 66% of precipitation. Alpine *ET* was greatest during the winter, in part because of sublimation from blowing snow, which contributed from 27% to 48% of the alpine, and 6% to 9% of the catchment water balance, respectively. The subalpine *ET* peaked in summer. Alpine areas generated the majority of the catchment discharge, despite covering only 31% of the catchment area. Although the average annual alpine runoff efficiency (discharge/precipitation; 40%) was greater than the subalpine runoff efficiency (19%), the subalpine runoff efficiency was more sensitive to changes in precipitation. Inter-annual analysis of the evaporative and dryness indices revealed persistent moisture limitations at the catchment scale, although the alpine alternated between energy-limited and water-limited states in wet and dry years. Each ecosystem generally over-generated discharge relative to that expected from a Budyko-type model. The alpine and catchment water yields were relatively unaffected by annual meteorological variability, but this interpretation was dependent on the method used to quantify potential *ET*. Our results indicate that correctly accounting for dissimilar hydrological cycling above and below alpine treeline is critical to quantify the water balance of high-elevation mountain catchments over periods of meteorological variability. Copyright © 2015 John Wiley & Sons, Ltd.

KEY WORDS water balance; Budyko; PET; snowmelt; blowing snow; Niwot Ridge

Received 26 May 2014; Accepted 28 April 2015

INTRODUCTION

The hydrology of the intermountain western United States, like many semi-arid regions of the world, is dominated by snowmelt runoff (Serreze *et al*., 1999). In general, climate models forecast increased air temperatures for this region (Rasmussen *et al*., 2011), and this is predicted to result in a decreased annual snow pack, earlier onset of snowmelt, and a higher percentage of precipitation as rain *versus* snow (Stewart *et al*., 2005; Knowles *et al*., 2006; Clow, 2010; Harpold *et al*., 2012), which could alter the timing, duration, and amount of snow accumulation in mountain catchments (Nayak *et al*., 2010). These changes may in turn affect patterns of discharge, evapotranspiration (*ET*), and water availability.

Hydro-climatological modelling of mountain ecosystems suggests that they may become more water stressed in the future (e.g. Tague *et al*., 2009; Tague and Peng, 2013). However, a limitation of regional-to-global scale models is that they typically perform poorly in snow-dominated mountainous watersheds such as those in the Colorado Front Range (Rasmussen *et al*., 2011). Additional errors can be introduced when large-scale models are statistically or dynamically downscaled, especially over complex terrain (e.g. French *et al*., 2003; Gutmann *et al*., 2012). For these reasons, it is critical to use direct measurements to support hydro-climatological modelling efforts in mountain areas, both to accurately characterize hydrological fluxes in complex terrain, and to constrain and verify modelling results (Kane and Yang, 2004; Hong *et al*., 2009).

High-elevation mountain areas are generally water-rich but data-poor (Beniston *et al*., 1997). There is also a growing need to conduct detailed studies of water

*Correspondence to: John F. Knowles, Department of Geography, University of Colorado, UCB 260, Boulder, CO 80309-0260, USA
E-mail: John.Knowles@Colorado.edu
†Now at the Department of Natural Resources

balances in semi-arid regions such as the Rocky Mountains, where both changing climate and population growth are increasing the demand on water resources (Vörösmarty *et al*., 2000; Mackun and Wilson, 2011). In Colorado, the 3100 to 3700 m a.s.l. elevation range is designated as the most important for generating snowmelt runoff (Segura and Pitlick, 2010), but logistical constraints generally restrict data collection to a campaign basis in these seasonally snow-covered areas, and accurate measurements of snowfall are difficult to obtain (Williams *et al*., 1999; Rasmussen *et al*., 2012). Moreover, this elevation range is transected by treeline, which is located between 3400 and 3600 m a.s.l. in Colorado (Elliott, 2011). This important elevation range for generating snowmelt runoff is thus divided into alpine and subalpine zones, where contrasting hydrological processes complicate the partitioning of precipitation into discharge and *ET* (Seastedt *et al*., 2004; Molotch *et al*., 2007; Blanken *et al*., 2009; Knowles *et al*., 2014).

Catchment-scale discharge provides a good opportunity to address these problems within the Budyko framework (Budyko, 1974), where the partitioning of precipitation between *ET* and discharge is treated as a functional balance between the supply of and demand for water by the atmosphere (Roderick and Farquhar, 2011). This requires knowledge of both *ET* and potential evapotranspiration (*PET*), each of which requires special consideration to accurately quantify in mountain environments. Although the eddy covariance technique has become an increasingly common and effective way to measure *ET* in mountain ecosystems (e.g. Goulden *et al*., 2012; Knowles *et al*., 2014), the choice of a particular *PET* model depends on the dominant environmental controls on the system of study, and also on which data are available (Fisher *et al*., 2010). Air temperature-based approaches to calculate *PET* are simple and therefore widely applicable (Yao and Creed, 2005), but they often underestimate *PET* (Yao, 2009). Like air temperature-based models, radiation-based models do not explicitly account for atmospheric demand apart from energy supply, and by assuming that the surface is extensive and continually saturated, omit the effects of advective variables such as wind speed and humidity (Donohue *et al*., 2010). Alternatively, physical *PET* models that incorporate measures of humidity and wind speed (e.g. Penman) are nearly universally applicable (although they are relatively data intensive), and recent work recommends the Penman model over both air temperature-based and radiation-based models for application in semi-arid environments provided the availability of high-quality meteorological forcing data (e.g. Donohue *et al*., 2010; Fisher *et al*., 2010; McAfee, 2013).

Despite decades of catchment water balance studies, rarely are there sufficient internal measurements to partition precipitation, *ET*, and discharge (both measured and as a residual), and to compare and contrast the performance of *PET* methods, from above-treeline and below-treeline ecosystems within a single catchment. Accordingly, we utilized a heavily instrumented research catchment to (1) separately evaluate the hydrological fluxes of precipitation, *ET*, discharge, and *PET* from subalpine forest and alpine tundra ecosystems; (2) calculate the mean annual catchment water balance between 1 October 2008 and 30 September 2012; and (3) characterize periods of energy *versus* water limitation within the Budyko framework, in order to improve our understanding of how water partitioning responds to inter-annual meteorological variability at both the ecosystem and the catchment scale. We hypothesize that water partitioning will be more sensitive to inter-annual precipitation variability (and less sensitive to atmospheric water demand) in the alpine compared to the subalpine ecosystem because of the relative inability of alpine areas to adjust *ET* to compensate for meteorological variability (Jones *et al*., 2012; Creed *et al*., 2014).

METHODS

Site description

The Como Creek catchment is located on and below the southeast flank of Niwot Ridge (40°N, 105°W) in Colorado, USA, approximately 4–9 km east of the Continental Divide. The catchment is 5.36 km^2 in area and ranges in elevation from 2900 to 3560 m a.s.l. (Figure 1). This region was glaciated during the Pleistocene, and the catchment is primarily characterized by Precambrian siliceous metamorphic and granitic bedrock (Murphy *et al*., 2003). The lower boundary of the catchment is situated on top of the ~10-m thick Arapaho moraine (Gable and Madole, 1976). The soils are Inceptisols intermixed with Alfisols, 30–60 cm deep in areas absent of glacial till, and 60–100 cm deep on the moraine (Lewis and Grant, 1979). We used a LiDAR-derived 2-m digital elevation model from the Niwot Ridge Long-Term Ecological Research (LTER) Program spatial data set (http://culter.colorado.edu) and standard GIS catchment delineation tools to show that approximately 69% (3.72 km^2) of the catchment is located below treeline and 31% (1.64 km^2) above treeline (Figure 1). The forested portion of the catchment was logged at the turn of the 20th century, but has seen minimal human disturbance since that time (Lewis and Grant, 1979). The conifer-dominated forest (leaf-area index ~ 4.2 $m^2\,m^{-2}$ near the US-NR1 AmeriFlux tower; Turnipseed e*t al*., 2002) is currently dominated by Engelmann spruce (*Picea engelmannii*), subalpine fir (*Abies lasiocarpa*), limber pine (*Pinus flexilis*),

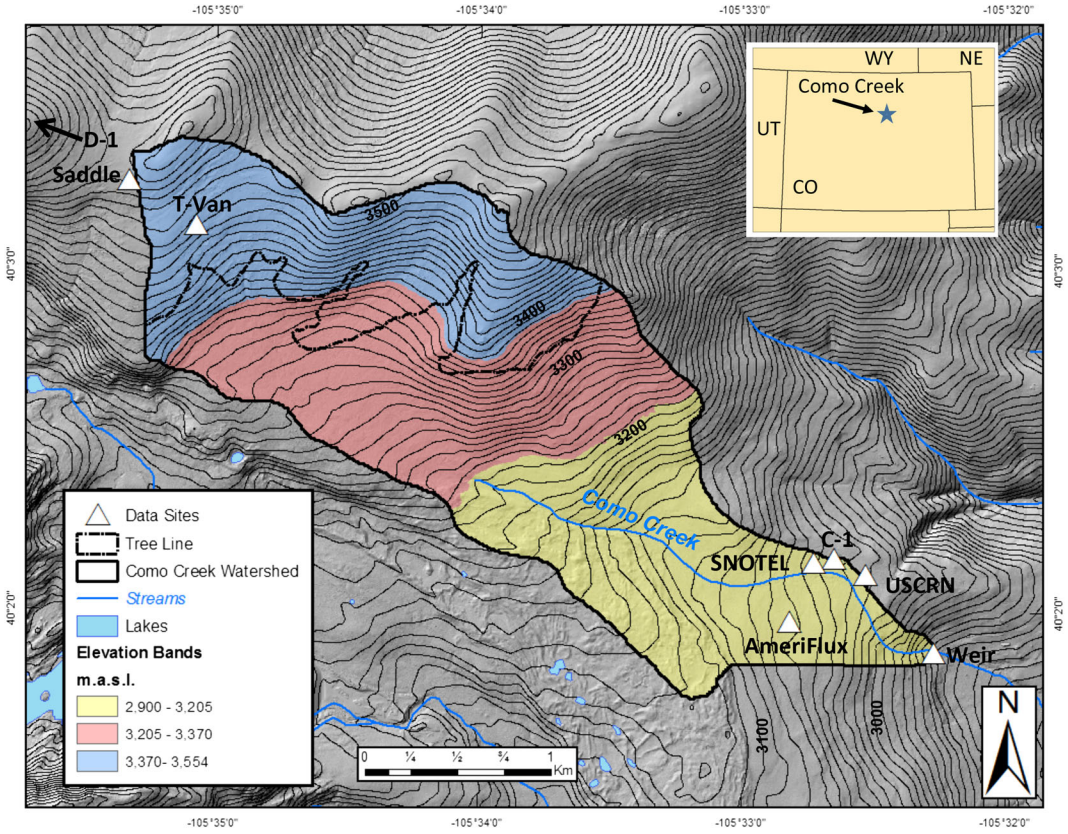

Figure 1. Map of the Como Creek catchment showing all sampling locations. The catchment has an area of 5.36 km^2 with approximately 31% and 69% of the catchment above and below treeline, respectively. Three distinct elevation bands were generated by the Jenks Natural Breaks classification method to spatially distribute precipitation across the catchment. Insert shows the regional location of the catchment

lodgepole pine (*Pinus contorta*), and, to a lesser extent, quaking aspen (*Populus tremuloides*) (Burns *et al*., 2014). Tundra vegetation is found in alpine areas where specific vegetation communities are chiefly dependent on moisture availability (Walker *et al*., 2001); dry meadow communities are dominant in this catchment (Darrouzet-Nardi *et al*., 2012).

Between the 2010 and 2012 water years (1 October to 30 September), snow accounted for between 63% of annual precipitation at the lower end of the catchment and 75% of annual precipitation at the headwaters of the catchment, following standard National Atmospheric Deposition Program protocols for precipitation type classification (Williams *et al*., 2011). Summer precipitation typically occurs during afternoon convective storms, which can bring intense but sporadic rainfall (Greenland and Losleben, 2001). Winter is windy, with the above-canopy winter wind speed averaging 7 and 13 $m\,s^{-1}$ at subalpine and alpine sites, respectively (Blanken *et al*., 2009). The alpine portion of the catchment is windier than the adjacent Green Lakes Valley catchment (1998–2000 mean winter wind speed = 8 $m\,s^{-1}$; Niwot LTER unpublished data) because of greater exposure. Because of this exposure, snow deposition in the alpine is primarily controlled by topography relative to the prevailing westerly winds, and the largest accumulation zones occur in leeward depressions and sheltered areas (Hood *et al*., 1999; Erickson *et al*., 2005; Darrouzet-Nardi *et al*., 2012).

We utilized hydrological and climatological data for this study collected from eight locations, including a weir at the catchment outlet, four sites within the lower, subalpine part of the catchment (C-1, the United States Climate Reference Network (USCRN) site Boulder 14W, the Niwot snow telemetry (SNOTEL) site, and the US-NR1 AmeriFlux tower), and three alpine meadow sites within (T-Van), adjacent to (Saddle), or above (D-1) the upper part of the catchment (Figure 1), to calculate the annual alpine, subalpine, and catchment water balances between water years 2008 and 2012. Table I includes the make and model numbers of the instruments at each location. The weir, C-1, T-Van, Saddle, and D-1 locations operate as part of the Niwot Ridge LTER Program, which has recorded continuous meteorological measurements since 1953 (C-1 and D-1; Williams *et al*., 1996). Data from these sites can be downloaded through the Niwot Ridge LTER database (http://culter.colorado.edu/NWT). Data from the Niwot Ridge US-NR1 AmeriFlux tower (we used version 2013.02.28) are available at http://ameriflux.ornl.gov,

Table I. Location, elevation, make, and model of the instruments used to measure the fluxes of the water balance and *PET*, including units and systematic measurement uncertainty

Location	Elevation (m a.s.l.)	Ecosystem type	Measurement	Units	Instrument	Range of systematic uncertainty
Catchment outlet	2900	Subalpine forest	Stage height	cm	Solinst Barologger gold pressure transducer	±5.7% of discharge (calibration)
			Stream velocity	$m\,s^{-1}$	Marsh McBirney model 201D	±5.7% of discharge (calibration)
USCRN Boulder 14W	2996	Subalpine forest	Precipitation	mm	Shielded Geonor T-200B	±0.1% (factory)
Niwot SNOTEL	3021	Subalpine forest	Precipitation	mm	Sensotec 100" pressure	±2.5% (estimate)
			Snow-water equivalent	mm	transducer	±2.5% (estimate)
C-1	3023	Subalpine forest	Precipitation	mm	Shielded Belfort 5–780	±2% (calibration)
Niwot AmeriFlux	3050	Subalpine forest	Wind speed	$m\,s^{-1}$	Campbell Scientific CSAT3 sonic anemometer	±0.08 $m\,s^{-1}$ (factory)
			Water vapour density (primary)	$g\,m^{-3}$	Campbell Scientific KH2O open-path krypton hygrometer	±10% of co-located LI-6262 H_2O flux (calibration)
			Water vapour density (secondary)	$g\,m^{-3}$	LI-COR LI-6262 closed-path infrared gas analyser	±10% of co-located KH2O H_2O flux (calibration)
			Air temperature	°C	Vaisala HMP35D	±0.4 °C (factory)
			Vapour pressure deficit	kPa	Vaisala HMP35D	±2% (factory)
			Net radiation	$W\,m^{-2}$	REBS Q-7.1	−2–4% (calibration)
			Soil heat flux	$W\,m^{-2}$	REBS HFT-1	±5% (estimate)
Niwot T-Van	3480	Alpine tundra	Wind speed	$m\,s^{-1}$	Campbell Scientific CSAT3 sonic anemometer	±0.08 $m\,s^{-1}$
			Water vapour density	$g\,m^{-3}$	LI-COR LI-7500 open-path infrared gas analyser	±10% of H_2O flux (estimate)
			Air temperature	°C	Vaisala HMP45C	±0.4 °C (factory)
			Vapour pressure deficit	kPa	Vaisala HMP45C	±2% (factory)
			Net radiation	$W\,m^{-2}$	Kipp and Zonen NR Lite	−2–4% (calibration)
			Soil heat flux	$W\,m^{-2}$	REBS HFT-3	±5% (factory)
Niwot Saddle	3528	Alpine tundra	Precipitation	mm	Shielded Belfort 5–780	+61% during winter (calibration)
D-1	3729	Alpine tundra	Precipitation	mm	Shielded Belfort 5–780	±2% (calibration)

We performed all sensor calibrations except for the net radiometers where the uncertainty was estimated from Blonquist *et al*., 2009, and the Belfort precipitation gages that were calibrated according to Williams *et al*. (1998) (Saddle) and Wetherbee *et al*. (2013) (C-1 and D-1)

PET, potential evapotranspiration; USCRN, United States Climate Reference Network; SNOTEL, snow telemetry

Niwot SNOTEL data can be found at http://www.wcc.nrcs.usda.gov/nwcc/site?sitenum=663&state=co, and USCRN data are at http://www.ncdc.noaa.gov/crn/qcdatasets.html. Throughout the manuscript, statistical comparisons were evaluated using Student's two-tailed *t*-test, and we use $p < 0.10$ as a breakpoint for significance (Barlow, 1989).

Precipitation

Precipitation measurements were collected at three subalpine locations (Table I) and then averaged on an annual basis to determine representative precipitation amounts for the subalpine portion of the catchment. These three precipitation datasets were continuous throughout the length of the observation period, except the Niwot SNOTEL gage, which developed a leak in 2008, and no measurements were taken between 23 May and 30 September of that year (personal communication, 19 July 2012, M. Skordahl, NRCS). During that period, data were gap filled using the long-term relationship between the Niwot and University Camp (3160 m a.s.l.; 3 km southwest of Niwot) SNOTEL stations. Alpine precipitation was measured at the Saddle and D-1, and Saddle precipitation was corrected for overcatch from blowing snow during non-precipitation events following the method of Williams *et al.* (1998).

We used a hypsometric method (Dingman, 2002) to spatially distribute precipitation amount across the entire catchment, using data from five stations across a range of 733 vertical metres (Table I). Precipitation was calculated by summing daily data to generate an annual total by water year for each site. A unique hypsometric curve was established for each water year by linear regression of summed precipitation against station elevation ($0.77 < R^2 < 0.99$):

$$P(z) = az + b \tag{1}$$

where the dependent variable P (precipitation) is a function of elevation (z) in metres, and a and b are the slope and the y-intercept of each unique linear regression. To calculate z, the total drainage area was divided into three elevation bands by application of the Jenks Natural Breaks classification method (Jenks, 1967) to the catchment digital elevation model using ArcMap. The Jenks Natural Breaks method separates the topography of the catchment into distinct classes (elevation bands) by minimizing the variance within classes, while maximizing the variance among classes. We calculated the mean z and the area of each elevation band relative to the total area of the catchment (a_h), and then the total precipitation amount for each band was determined using Equation (1), multiplied by the corresponding a_h, and summed to generate a value for the entire catchment:

$$\hat{P} = \sum_{h=1}^{H} P(z) a_h \tag{2}$$

where h is elevation band, H is the number of elevation bands, and $\hat{P}$ is total catchment precipitation.

Evapotranspiration

Measurements of *ET* represent the aggregated measurements of evaporation, transpiration, and sublimation. The *ET* data were calculated from water vapour fluxes measured via the eddy covariance method at both the Niwot Ridge US-NR1 AmeriFlux tower (subalpine forest; Turnipseed *et al.*, 2002) and near T-Van (alpine tundra; Knowles *et al.*, 2012). In the subalpine, an open-path krypton hygrometer [measurement height = 21.5 m above ground level (a.g.l.)] was used to measure the water vapour density, and an open-path infrared gas analyser (measurement height = 3 m a.g.l.) was used at T-Van. Both sites used a three-dimensional sonic anemometer to measure vertical wind fluctuations (Table I). Water vapour fluxes were calculated from the covariance between the vertical wind speed and water vapour density fluctuations (e.g. Foken *et al.*, 2012). Post-processing of the eddy covariance data consisted of standard corrections including coordinate rotation and Webb adjustment following Lee *et al.* (2004). The monthly net *ET* flux was calculated from the cumulative sum of measurements taken at 30-min intervals. We also considered sublimation of snow from blowing snow in the alpine portion of the catchment (e.g. not measured by eddy covariance); details of this calculation can be found in Knowles *et al.* (2012). The resulting additional *ET* from the sublimation of blowing snow was added to the measured alpine *ET* to produce total alpine *ET* (Table II).

To spatially distribute *ET* fluxes across the catchment, we applied the US-NR1 AmeriFlux tower data to the area below treeline and the T-Van data to the area above treeline and thereby assumed that flux measurements obtained from each flux tower characterized the overall response of the ecosystem under study (Hollinger *et al.*, 2004). This common assumption is based on the fact that the upwind sample area, or 'footprint', of measured fluxes integrates over a distance of ~400 m (T-Van) to ~1200 m (US-NR1) (Blanken *et al.*, 2009), which allows the evaluation of processes at the ecosystem scale (Baldocchi *et al.*, 2000). This can be particularly advantageous in alpine areas, where small-scale topographical complexity can result in significant changes in snow cover, resultant soil moisture, and *ET* (Knowles *et al.*, 2012).

Estimates of annual *PET* values were calculated from daily meteorology using air temperature-based (Hamon), radiation-based (Priestley–Taylor), and physical (Penman) approaches (Penman, 1948; Hamon, 1963; Priestley and

Table II. Fluxes of the alpine, subalpine, and catchment water balances, including the mean, standard deviation, and systematic uncertainty

Subalpine forest

Water year	P (mm)	Q^* (mm)	Q efficiency (%)	ET (mm)
2008	761	140	18	621
2009	696	103	15	593
2010	703	127	18	576
2011	889	265	30	624
2012	704	83	12	621
Mean	751	144	19	607
Std dev	82	71	7	21
Uncertainty	26	66	9	61

Alpine tundra

Water year	P (mm)	Q^* (mm)	Q efficiency (%)	Measured ET (mm)	Blowing snow ET (mm)	Total ET (mm)
2008	1170	509	44	399	262	661
2009	866	264	30	415	187	602
2010	937	350	37	385	202	587
2011	1527	746	49	414	367	781
2012	860	334	39	360	166	526
Mean	1072	441	40	395	237	631
Std dev	284	193	7	23	81	96
Uncertainty	21	67	6	39	24	63

Catchment

Water year	P (mm)	Q (mm)	Q efficiency (%)	ET (mm)	ΔS (mm)	ΔS (%)
2008	955	175	18	633	147	15.4
2009	841	194	23	596	51	6.1
2010	855	238	28	579	38	4.4
2011	1198	327	27	672	199	16.6
2012	800	131	16	592	77	9.7
Mean	930	213	23	614	102	10.4
Std dev	160	74	5	38	69	5.4
Uncertainty	33	12	4	88	95	10.2

The P is measured precipitation, Q is measured discharge, Q efficiency is Q/P, ET is measured evapotranspiration, Q^* is $P - ET$, Q^* efficiency is Q^*/P, and ΔS is storage calculated as $P - (Q + ET)$. The alpine ET is divided into measured and blowing snow-derived ET to emphasize the importance of blowing snow to winter sublimation
Std dev, standard deviation

Taylor, 1972). We quantified Hamon *PET* following Lu *et al*. (2005) as follows:

$$PET = 0.1651 * L_d * \rho_{sat} * K_{CPE} \tag{3}$$

where L_d is the daytime length in hours as a function of latitude, ρ_{sat} is the saturated vapour density ($g\,m^{-3}$) at the daily mean air temperature, and K_{CPE} is the calibration coefficient (1.2) used to adjust *PET* calculated from Hamon (1963) to realistic values (Lu *et al*., 2005) given that K_C is a crop coefficient and subscripted *PE* denotes potential evaporation. Priestley–Taylor *PET* was calculated following Shuttleworth (1993):

$$PET = \alpha \frac{\Delta}{\Delta + \gamma}(R_n - G) \tag{4}$$

where α is the Priestley–Taylor coefficient (1.26), Δ is the rate of increase of saturation vapour pressure with air temperature, γ is the psychrometric constant $\left(\frac{C_p P}{\varepsilon \lambda}\right)$, C_p is the specific heat of moist air at constant pressure ($1.013\,kJ\,kg^{-1}\,°C^{-1}$), P is the atmospheric pressure (kPa), ε is the ratio of the molecular weight of water vapour to that of dry air (0.622), λ is the latent heat of vapourization of water ($2.501\,MJ\,kg^{-1}$), R_n is measured net radiation, and G is the measured soil heat flux. Penman *PET* was also calculated (constants developed for an open water surface) following Shuttleworth (1993):

$$PET = \frac{\Delta}{\Delta + \gamma}(R_n - G) + \frac{\gamma}{\Delta + \gamma}\frac{6.43(1 + 0.536U)D}{\gamma} \tag{5}$$

where U is horizontal wind speed ($m\,s^{-1}$) and D is vapour pressure deficit (kPa).

Discharge

The water level in Como Creek was measured with a pressure transducer at a weir located at the catchment

outlet (Figure 1) and converted to volumetric discharge using empirical rating curves unique to each water year ($0.90 < R^2 < 0.97$). The discharge was calculated as a power function:

$$Q = aX^b \tag{6}$$

where Q is discharge in litres per second, X is the stage height in centimetres, and a and b are constants derived from a power curve fitted to the plot of stage height *versus* discharge. Weekly measurements of stage and velocity (Table I) were used to create the empirical rating curves for each water year. The pressure transducer was installed each year in April and removed in early November because of freezing in the stilling well. To account for winter flows, a baseflow value of $3\,\mathrm{L\,s^{-1}}$ was applied during the winter months [day of year (DOY) 315 to DOY 115], which amounted to 45% of the year, but only an average of 4% of the total annual flow. This value was chosen based on late season (baseflow) transducer values, occasional manual measurements during winter months, and earlier work that reported winter flow of $3\,\mathrm{L\,s^{-1}}$ using a flume at a nearby location on Como Creek (Lewis and Grant, 1979). When the transducer record began after DOY 115 or ended prior to DOY 315, daily discharge values were linearly interpolated to baseflow values at the beginning or end of the year (24% of values). The 5-day running mean discharge was used to gap fill missing values (4% of values). Volumetric discharge was divided by catchment area to convert to specific discharge and then reported as a depth of water (in mm) over the entire catchment. We also modelled ecosystem discharge as the residual of precipitation minus *ET* for both subalpine and alpine portions of the catchment (Table II). Although we recognize that this calculation assumes 100% water balance closure, it allows for comparison between water partitioning at the ecosystem scale. Significant correlation ($p = 0.08$; $R^2 = 0.70$) resultant from linear regression of measured annual catchment discharge (independent variable) against catchment discharge modelled as precipitation minus *ET* (dependent variable) provided justification for this approach.

Water balance

Measured hydrological fluxes were used to calculate the catchment water balance on a water-year basis and to determine water storage within the catchment as a residual:

$$\Delta S = P - (Q + ET) \tag{7}$$

where ΔS is the change in storage (Creutzfeldt *et al.*, 2014). We did not apply Equation (7) at the ecosystem scale because of the lack of ecosystem-specific discharge measurements.

Budyko analysis

We calculated the evaporative index (*ET*/*P*) as a function of the dryness index (*PET*/*P*) at the ecosystem and catchment scale to compare with Budyko-modelled water partitioning estimates (Budyko, 1974):

$$\frac{ET}{P} = \left[\phi \tan^{-1}(1/\phi)\left(1 - \exp^{-\phi}\right)\right]^{0.5} \tag{8}$$

where ϕ is the dryness index, which provides a measure of energy (dryness index < 1) *versus* moisture (dryness index > 1) limitation. For this analysis, we calculated catchment *ET* as both the eddy covariance-measured, area-weighted ecosystem *ET* and *ET* estimated from the water balance (*ET** = precipitation minus discharge). Points that fall above the Budyko curve correspond to higher-than-predicted *ET* and lower-than-predicted discharge, while points that fall below the curve represent lower-than-predicted *ET* and higher-than-predicted discharge. The annual discharge anomaly was equal to the difference between measured (or modelled) annual discharge and Budyko-predicted discharge, divided by precipitation (Berghuijs *et al.*, 2014).

The elasticity metric further provides a measure of water partitioning as a function of hydro-climatic variability, and we calculated elasticity following Creed *et al.* (2014) as the ratio of the inter-annual range in dryness index values to the range of the evaporative index residual values (measured evaporative index minus Budyko-modelled evaporative index). Greater elasticity corresponds to more resilient water yields (e.g. water partitioning between discharge and *ET* less affected by changing climate) and vice versa.

Measurement uncertainty

Measurement uncertainty stems from a combination of random and systematic uncertainty, where random uncertainty is analogous to measurement precision, and systematic uncertainty affects measurement accuracy (Taylor, 1997). When possible, we used either site-specific or factory calibrations to determine the systematic uncertainty of individual measurements; in the absence of calibration, systematic uncertainty was estimated via expert opinion (Table I). We then applied the standard error propagation formula (Taylor, 1997) to quantify the nonlinear effect of systematic error propagation through the various formulae used in the calculation of the water balance (Graham *et al.*, 2010):

$$\delta_s q = \sqrt{\sum_{n=1}^{N}\left(\frac{\partial q}{\partial x_n}\delta_s x_n\right)^2} \tag{9}$$

where q is a function of N variables (x) and $\delta_s q$ is the systematic error propagated through q. The daily

systematic measurement error was then aggregated on an annual basis (Moncrieff *et al.*, 1996):

$$\eta = \sqrt{\left(\sum_{t=1}^{T} \frac{\partial q}{\partial x_n} \delta_s x_t\right)^2} \tag{10}$$

for variable x from time $1:T$ to produce the annual systematic uncertainty (η) values in Table II. Because random uncertainty diminishes when aggregated to longer periods and larger areas according to $1/\sqrt{T}$ (Barlow, 1989), we assumed that errors due to random measurement uncertainty cancelled out on an annual basis, and we did not propagate or aggregate random uncertainty through our results.

RESULTS

Water balance fluxes

The Jenks Natural Breaks method generated three distinct elevation bands with mean elevations of 3108, 3286, and 3443 m a.s.l., which represented 33%, 36%, and 31% of the total catchment area, respectively (Figure 1). The annual catchment precipitation ranged between 800 and 1198 mm, and the catchment mean annual precipitation (*MAP*) was 930 mm ($\eta = 33$ mm) (Table II). The subalpine *MAP* was 751 mm ($\eta = 26$ mm), and the alpine *MAP* was 1072 mm ($\eta = 21$ mm). Neither the subalpine nor the alpine *MAP* was significantly different than the long-term average *MAP*, although the *MAP* was significantly different ($0.001 < p < 0.01$) between all three subalpine precipitation gages. There was a significant ($p = 0.09$) linear relationship between elevation and precipitation in winter (October to April), but no relationship in summer (May to September). Over the entire 5 years, precipitation increased 74 mm per 100-m increase in elevation.

The *ET* was the largest water output, and the mean annual catchment *ET* was 614 mm ($\eta = 88$ mm), or 66% of *MAP* (Table II). Overall, mean annual alpine *ET* (631 mm; $\eta = 63$ mm) and subalpine *ET* (607 mm; $\eta = 61$ mm) were similar. The catchment *ET* remained nearly constant throughout the year because of the seasonally inverse timing between peak *ET* fluxes from subalpine and alpine areas. The greatest difference between subalpine and alpine *ET* was in summer when the subalpine *ET* was much greater as a result of more transpiration (Moore *et al.*, 2008). The subalpine *ET* exceeded precipitation during the summer, consistent with previous results using the Thornthwaite–Mather technique (Thornthwaite and Mather, 1957; Greenland, 1989). The *ET* was less than precipitation during all other seasons.

During the winter, sublimation from alpine areas was important because of both greater wind speed and greater snowfall relative to the subalpine, and this promoted both *in situ* sublimation and also sublimation of blowing snow in suspension (Tabler, 2003; Knowles *et al.*, 2012). The mean winter *in situ* sublimation flux was 180 mm to which we added an average of 237 mm additional sublimation from blowing snow. As a result, winter *ET* fluxes accounted for 66% of total alpine *ET*, but only 41% of total subalpine *ET*. During a period of concurrent data collection (water years 2008 through 2010), the average magnitude of the alpine winter *ET* flux (424 mm including blowing snow) was 30% greater than the corresponding *ET* flux (325 mm) calculated using the aerodynamic profile method over a seasonal snowpack at a more sheltered location approximately 500 m northwest of T-Van (Niwot Subnivean Lab; Niwot Ridge LTER unpublished data). Combining the subalpine and alpine ecosystems, Penman *PET* was 1.8 times greater than Priestley–Taylor *PET* and 3.0 times greater than Hamon *PET* (Table III). In the subalpine, the *PET* variability (standard deviation) was similar between *PET* methods, whereas the alpine Penman *PET* was 7.1 and 9.5 times more variable than the alpine Hamon and Priestley–Taylor *PET*, respectively.

Over the entire catchment, the mean annual runoff efficiency (discharge/precipitation) was 23%, and the mean annual specific discharge was 213 mm ($\eta = 12$ mm). The modelled (as precipitation minus measured *ET*) runoff efficiency was greater in alpine relative to subalpine areas, and weighted by land area, the alpine also contributed disproportionately to catchment discharge (Figure 2). Specifically, alpine areas contributed between 54% and 64% of the catchment discharge although they accounted for only 31% of the catchment land area. The subalpine runoff efficiency increased 7.9% for every 100 cm precipitation ($p < 0.001$) relative to a corresponding 2.0% increase in the alpine ($p = 0.05$; Figure 3). Total annual inputs (precipitation) were greater than outputs (discharge and *ET*), and the mean annual ΔS was 102 mm ($\eta = 95$ mm), or 10.2% of *MAP* (Table II).

Snowmelt variability

The inter-annual magnitude and timing of peak snow-water equivalent (*SWE*) in the subalpine forest varied by 153 mm and 78 days between the wettest (2011) and driest (2012) winters (Figure 4a). The duration of snowmelt, or the amount of time between peak and zero *SWE*, ranged from 22 (2011) to 73 (2012) days, and the catchment runoff efficiency was greatest when melt was fastest and least when melt was slowest. The spring snowmelt pulse generally dominated the annual hydrograph (Figure 4b), and between 2008 and 2011,

Table III. Comparison of three different methods used to calculate *PET* for Budyko analysis

Subalpine forest					
Method	Mean	Std dev	*CV*	*Q** elasticity	*Q** anomaly
Hamon	474	18	0.04	2.9	−0.29
Priestley–Taylor	971	31	0.03	3.9	−0.03
Penman	1297	26	0.02	2.7	0.16
Alpine tundra					
Method	Mean	Std dev	*CV*	*Q** elasticity	*Q** anomaly
Hamon	394	10	0.03	2.1	−0.25
Priestley–Taylor	460	13	0.03	2.3	−0.21
Penman	1267	95	0.07	16.0	0.34
Catchment					
Method	*Q* elasticity	*Q** elasticity	*Q* anomaly	*Q** anomaly	
Hamon	4.2	1.4	−0.20	−0.30	
Priestley–Taylor	9.7	2.9	−0.02	−0.13	
Penman	5.4	3.5	0.13	0.03	

Meteorological inputs for the various methods are listed in Evapotranspiration section. Units for the mean and standard deviation (Std dev) of *PET* are millimetres; the coefficient of variation (*CV*), elasticity, and anomaly values are ratios. The *Q* is measured discharge and *Q** is modelled (*P* – *ET*) discharge

PET, potential evapotranspiration

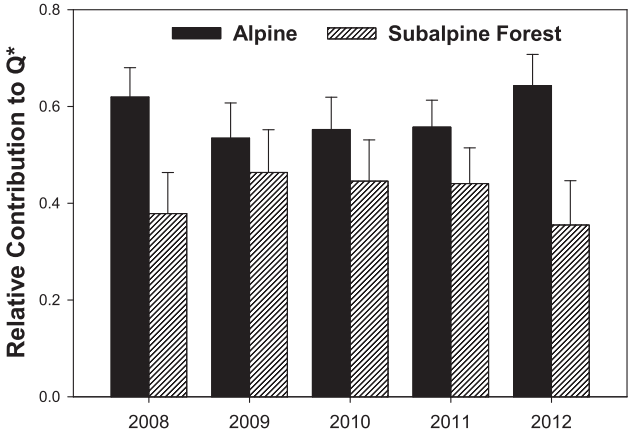

Figure 2. The relative contributions of alpine and subalpine areas to catchment *Q** (precipitation minus *ET*) over time. Error bars correspond to the propagated systematic measurement uncertainty

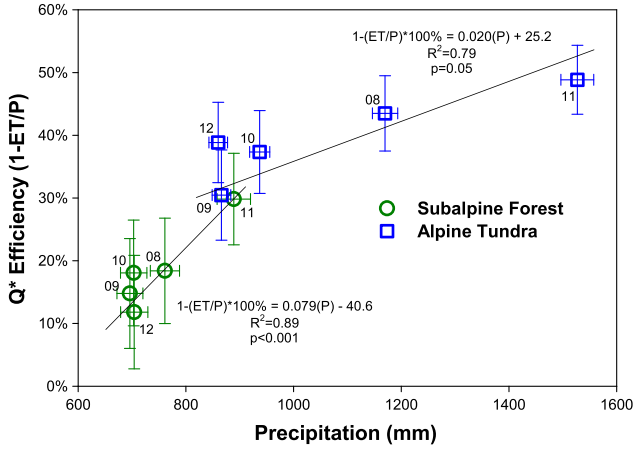

Figure 3. The subalpine forest and alpine tundra *Q** efficiency increases with precipitation (*P*). Lines represent the best-fit trendline resultant from ordinary least squares linear regression analysis, with corresponding equations, R^2, and *p*-values. Error bars correspond to the propagated systematic measurement uncertainty and numbers adjacent to each symbol indicate the water year

the timing of peak discharge varied by 19 days, from 1 June to 20 June. In 2012, however, when cumulative *SWE* was lowest, the discharge peak corresponded to rainfall (peak discharge on 7 July) and not snowmelt, which is rare for high-elevation catchments in the Rocky Mountains (Stewart *et al.*, 2004). The 2008 through 2010 hydrographs were relatively similar in terms of the shape and the timing of the snowmelt pulse (Figure 4b), compared with 2011 (the wettest year), when the snowpack was deeper and snowmelt occurred much later in the year, and 2012, when discharge peaked in summer. Peak discharge in 2011 was nearly an order of magnitude greater than the 2012 peak discharge, but the total specific discharge was only about 2.5 times greater.

Budyko analysis and metrics

We selected the Penman method to characterize *PET* for Budyko analysis because it was the only *PET* calculation that incorporated wind speed, and high wind speeds are characteristic of this catchment, and a common feature of mountain ecosystems in general (Barry, 2008; Blanken *et al.*, 2009). The elasticity and discharge anomaly values were highly dependent on the method used to calculate *PET* for Budyko analysis, and our inferences about the hydrological partitioning and resultant elasticity of each ecosystem changed along with

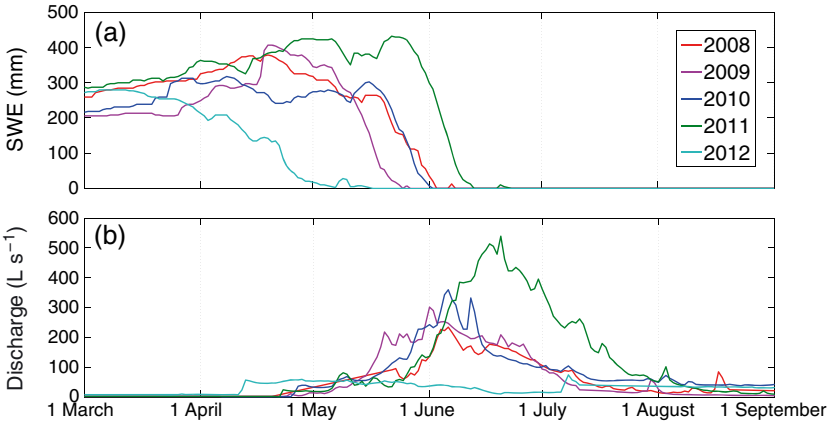

Figure 4. (a) The evolution of snow-water equivalent (SWE) at Niwot SNOTEL and (b) the catchment hydrograph for the period 1 March to 1 September for water years 2008 through 2012. Note that 2012 peak discharge occurred on 7 July after snowmelt

the method used to calculate *PET* (Table III). Using the Penman method, the mean annual elasticity ranged from 2.7 in the subalpine to 4.5 for the catchment and 16.0 in the alpine (Table III). While Hamon and Priestley–Taylor *PET* resulted in negative discharge anomalies for both ecosystems and the catchment, Penman *PET* discharge anomalies were positive. This result supports recent research suggesting that the discharge anomaly for a given catchment is directly proportional to the annual snowfall percentage (Berghuijs *et al.*, 2014). Using the Penman method, the discharge anomaly ranged from 0.13 at the catchment scale (using measured discharge) to 0.16 in the subalpine and 0.34 in the alpine (Table III).

We contrasted the mean annual evaporative index to the mean annual dryness index within the Budyko framework for the subalpine forest, alpine tundra, and the entire catchment (Figure 5). In the subalpine, the dryness index was always greater than unity, demonstrating that moisture limitation imposed the principal control on *ET*. The wettest year in the subalpine was located below the Budyko curve, indicating a disproportionate influence of discharge and diminished *ET*, while water partitioning generally followed the Budyko relationship in other years (points near the Budyko curve). The alpine dryness index spanned a large range from energy limitation in the wettest year to moisture limitation during drier years, and the alpine always over-generated discharge relative to the Budyko curve. The catchment was always moisture limited and over-generated discharge in all years (measured *ET*) or in select years (modelled *ET*) depending on the method used to quantify *ET*.

DISCUSSION

The study period encompassed a wide range of conditions, from near-record winter and spring snowfall (2011) to an exceptional early season drydown (2012), but the average and range of ΔS (i.e. difference between inputs and outputs) was similar to other water balance

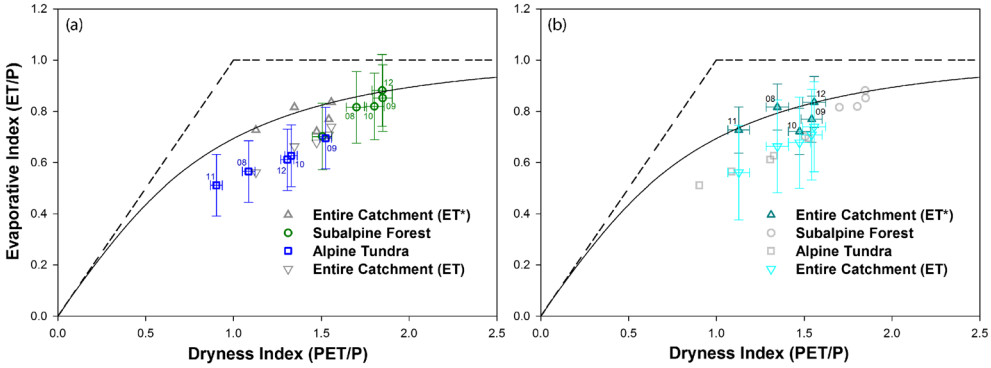

Figure 5. The annual evaporative index as a function of the dryness index is highlighted at the (a) ecosystem and (b) catchment scale from water years 2008 through 2012 (same data on each panel for comparison). Catchment *ET* is shown as both a measured (*ET*) and residual (*ET** = precipitation minus measured discharge) value. The theoretical Budyko relationship (solid line) and the physical limits to *ET* (dashed line) are also shown. The numbers adjacent to each symbol indicate the water year. The *PET* was calculated using the Penman method. Error bars correspond to the propagated systematic measurement uncertainty

investigations in comparable climatic and topographic settings (e.g. Flerchinger and Cooley, 2000; Janowicz *et al*., 2004; Vasilenko, 2004; Zhuravin, 2004; Bales *et al*., 2011; Chauvin *et al*., 2011). The ΔS could have resulted from changes in water stored in subsurface reservoirs of the unsaturated or saturated zones; however, previous water balance research in permafrost-free catchments has shown soil moisture storage to be negligible on an annual basis (e.g. Bales *et al*., 2011; Chauvin *et al*., 2011). Consequently, ΔS may reflect deep seepage of infiltrated precipitation to bedrock flowpaths (Graham *et al*., 2010), snow that is transported out of the catchment via blowing snow (Knowles *et al*., 2012), or systematic measurement uncertainty (Graham *et al*., 2010). Because we did not measure ecosystem discharge and were thus unable to calculate ecosystem ΔS using Equation (7), we also consider the catchment ΔS to represent the maximum ecosystem ΔS. Overall, ΔS increased with increasing precipitation, and precipitation was a significant predictor of ΔS ($p = 0.08$).

To what degree does the catchment water balance reflect ecosystem-specific hydrological processes?

Despite the inter-annual variability of precipitation, we consistently estimated greater runoff efficiency in the alpine *versus* the subalpine ecosystem. In spite of this, the alpine runoff efficiency was lower than has been reported for other alpine water balance studies (e.g. Stednick, 1981; Kattelmann and Elder, 1991; Cowie, 2010), which may have resulted from our measuring *ET* over a particularly snow-scoured location, differences in the methods used to calculate *ET* (measured *versus* modelled techniques), and/or overcompensating for sublimation from blowing snow. The overall catchment runoff efficiency (23%) was consistent with our interpretation that greater alpine runoff efficiency (40%; $\eta = 6\%$) balanced lower subalpine runoff efficiency (19%; $\eta = 9\%$) at the catchment scale. The catchment *ET* to precipitation ratio (66%) was less than has been measured over boreal (88%; Black *et al*., 1996) and subalpine (84%; this study) forests, greater than alpine grasslands (60%; Gu *et al*., 2008) and alpine tundra (59%; this study), and similar to a boreal peatland (65%; Peichl *et al*., 2013). Taken together, these results suggest that the water balances of catchments that span alpine treeline are highly dependent on the fraction of alpine *versus* subalpine land cover because of different processes governing discharge and *ET* in these ecosystems. Consequently, the ratio of above-treeline and below-treeline area has the potential to introduce nonlinearities into the catchment-scale hydrological response to future climate variability that are not well understood.

Previous work has shown that snow mass loss due to snowpack and blowing snow sublimation is a major component of the alpine water balance (Strasser *et al*., 2008; MacDonald *et al*., 2010; Knowles *et al*., 2012), and water losses due to the combination of these processes ranged between 27% and 48% of the alpine water balance and 6% to 9% of the catchment water balance. Abiotic factors were thus a major component of alpine *ET* and resulted in similar-magnitude *ET* fluxes from the subalpine in summer and the alpine in winter, despite different dominant processes. Accordingly, peak alpine and subalpine *ET* were seasonally out of phase, which contrasts with previous results from alpine-only, subalpine-only, and alpine/subalpine integrated catchments, where *ET* was always higher in summer relative to winter (Janowicz *et al*., 2004; Blanken *et al*., 2009). Although elevated winter *ET* was partially due to the strong winds that promoted blowing snow (Berg, 1986) and sublimation from snow-scoured areas (Knowles *et al*., 2012), greater *in situ* sublimation from snowpack-covered alpine areas moderated the winter *ET* difference between snow-scoured and snow-covered zones (Hood *et al*., 1999).

Trends towards lower 1 April *SWE* and increased summer precipitation have been identified in Colorado and may be indicative of future climate (Clow, 2010). Compared with the long-term LTER climate record, 2012 was anomalously warm and dry during the winter and spring, but had one of the wettest summers, resulting in the median subalpine precipitation of all 5 years, but the minimum alpine precipitation. As a result, summer precipitation may be able to compensate for below-average winter precipitation to a greater degree in the subalpine, because of the distinct meso-scale distribution of winter (orographic) and summer (convective) precipitation. Moreover, the subalpine runoff efficiency was especially sensitive to changes in precipitation, which could result in the subalpine forest having a disproportionate impact on catchment runoff efficiency given similar precipitation changes across both subalpine and alpine ecosystems in the future. Collectively, these results show that the magnitude of precipitation alone is not necessarily sufficient to indicate the catchment water balance for any given year, but instead, that the timing and resulting spatial distribution of precipitation must be considered together to accurately estimate runoff efficiency (e.g. Clow, 2010; Cowie, 2010).

Water partitioning and limiting factors on ET relative to the Budyko framework

This study took advantage of ecosystem-specific *ET* measurements from a highly studied research catchment to understand the processes driving catchment water balances and their sensitivity to climate variability. Both subalpine and alpine ecosystems systematically over-generated

discharge with respect to the Budyko relationship (positive discharge anomalies) (Berghuijs *et al*., 2014), but dry years in the subalpine were characterized by reduced discharge and runoff efficiency in place of reduced *ET*. This may be evidence of water that originates in alpine areas moving through the catchment to lower elevations via streamflow, shallow subsurface flow, or blowing snow, potentially increasing water availability and/or water use efficiency by vegetation at lower elevations.

Because multiple variables can influence trends in *PET*, it is preferable to use data-intensive methods, where the source(s) of uncertainty can be identified, rather than using simpler methods that could mask important trends (McAfee, 2013). As a result of this analysis, we suggest that researchers seeking to model *PET* from ecosystems characterized by high wind speeds (e.g. tundra, grassland, desert, and open water) use Penman *PET* or another method that explicitly treats wind speed, to avoid potentially underestimating *PET* (Table III). Furthermore, meta-analysis studies that apply air temperature-based (e.g. Jones *et al*., 2012; Creed *et al*., 2014) or radiation-based (e.g. Williams *et al*., 2012; Chen *et al*., 2013) *PET* to a variety of ecosystems may systematically underestimate *PET* from a subset of catchments as a function of wind speed and/or atmospheric water demand, biasing their results. It is especially noteworthy that differences in *PET* calculations can be sufficiently large to change the sign of the discharge anomaly (Table III; Berghuijs *et al*., 2014).

By comparing the evaporative and dryness indices, we were able to normalize for precipitation and meteorology (e.g. *PET*) to investigate the ecosystem-level sensitivity to climate change using the elasticity metric (Creed *et al*., 2014). When the Hamon and Priestley–Taylor methods were used to quantify *PET*, the catchment appeared to be more elastic than either the subalpine or alpine ecosystems on their own, suggesting that compensatory subalpine/alpine hydrological trends may act to buffer against future climate change at the catchment scale (Table III). When we calculated *PET* using the Penman equation, however, the catchment appeared to be less sensitive to climate variability than the subalpine forest, but more sensitive than the alpine tundra (Table III), and the high alpine elasticity resultant from this analysis implies that alpine water yields (at least from windy alpine sites) may be relatively unaffected by increasing air temperatures in the future. We explain the latter conclusion by way of our assumption that alpine *PET* is mainly driven by windy conditions that change little from year to year. As such, increasing atmospheric demand due to a warming climate may have less of an effect on alpine relative to subalpine ecosystems, because of the greater influence of wind on alpine *ET* and *PET* relative to subalpine ecosystems.

These results are noteworthy in the context of recent work that used Hamon *PET* to show that the elasticity of an alpine catchment adjacent to Como Creek (Green Lakes Valley) was among the lowest of any site included in the meta-analysis (0.33), and therefore that future warming should result in much larger alpine water yields (Creed *et al*., 2014). We also used Hamon *PET* to quantify alpine elasticity (Table III), but the resulting elasticity value was over six times greater than the Creed *et al*. (2014) study. We attribute this to the different morphology, vegetation cover, and resulting wind and snowpack regimes between these two neighbouring catchments, and also to the fact that we measured *ET*, while Creed *et al*. (2014) modelled *ET* as precipitation minus discharge. Accordingly, the relatively consistent nature of alpine *ET* relative to discharge in the Como Creek catchment (Table II) reduced the variability of the evaporative index (denominator of the elasticity equation), increasing the ecosystem elasticity. Our analysis uncovered a similar trend at the catchment scale: Elasticity was always greater when *ET* was measured *versus* modelled, especially when using the Hamon or Priestley–Taylor *PET* models (Table III). Together, these results imply that researchers should exercise caution when selecting *PET* models, and also when interpreting water balance partitioning within the Budyko framework, as results may vary significantly as a function of both *ET* and *PET*. Moreover, the application of Budyko-style analyses to smaller catchments or at non-climatological time scales may require special consideration of hydrological processes and/or partitioning (and the associated observations) unique to a given location or period to address these issues.

SUMMARY AND CONCLUSIONS

This study provides information about the magnitude and partitioning of catchment-scale water balance fluxes in a 5.36-km^2 catchment that spans alpine treeline, which can be used to inform water management decisions and/or calibrate water balance models in the future. We were able to use direct measurements, within the context of an uncertainty analysis, to show that outputs of *ET* and discharge from this catchment did not completely offset precipitation on an annual basis. We thus demonstrate that the assumption of water balance closure through the use of residual fluxes has the potential to mask important uncertainty and/or storage terms (e.g. not all water becomes discharge or *ET*), which could alter the interpretation of Budyko results. Ecosystem type influenced water yield, and the alpine contributed disproportionately to catchment discharge by area. A shift towards more summer and less winter precipitation could thus reduce catchment discharge and runoff efficiency because the majority of alpine precipitation occurs as winter snowfall. Blowing snow was a key component of alpine *ET*, which was the largest component of the alpine water

balance at this windy location, and a major contributor to the catchment water balance. Accordingly, researchers must take care when modelling *ET* and/or *PET*, as these processes can be more complicated than simple *PET* models commonly account for, especially above alpine treeline.

When we used Penman *PET* to calculate elasticity, we found that the alpine tundra was more elastic than either the subalpine forest or the catchment, which contradicted our original hypothesis that alpine water partitioning would be less elastic and more sensitive to inter-annual precipitation variability. This was due to the exceptional inter-annual regularity of alpine *ET*, much of which occurred during the winter when persistent downsloping winds bolstered sublimation. Therefore, we would expect water yields from less windy alpine catchments to show a greater response to inter-annual precipitation variability. Although catchment-scale water partitioning was persistently moisture limited, Budyko analysis showed that a wetter climate in the future might be capable of moving the catchment towards an energy-limited state. Results from this study underscore the potential for differences between the hydrological cycles of alpine and subalpine ecosystems that must be accounted for to quantify the catchment water balance when ecosystem transitions (e.g. alpine treeline) occur within a single, topographically confined catchment. We hope that water resource managers will note the disproportionate influence of alpine areas and the interconnectedness of alpine and subalpine systems when planning for the impacts of climate change on future water resources in mountain areas.

ACKNOWLEDGEMENTS

The research was supported by NSF grants DEB 0423662 and DEB 1027341 to the Niwot Ridge LTER and DOE-TES grant 7094866 to the US-NR1 AmeriFlux site. A. A. H. was additionally supported by NSF grant EAR 1144894. We wish to acknowledge the University of Colorado Mountain Research Station staff for their commitment to data collection, especially Kurt Chowanski. We also thank Dr Chris Graham for assisting with our measurement uncertainty analysis and Dr Hope Humphries for help with data management and processing. Constructive comments from three anonymous reviewers improved the final version of this manuscript.

REFERENCES

Baldocchi DD, Finnigan J, Wilson K, Paw U KT, Falge E. 2000. On measuring net ecosystem carbon exchange over tall vegetation on complex terrain. *Boundary-Layer Meteorology* **96**: 257–291.

Bales RC, Hopmans JW, O'Geen AT, Meadows M, Hartsough PC, Kirchner P, Hunsaker CT, Beaudette D. 2011. Soil moisture response to snowmelt and rainfall in a Sierra Nevada mixed-conifer forest. *Vadose Zone Journal* **10**: 786–799. DOI:10.2136/vzj2011.0001.

Barlow RJ. 1989. *Statistics. A Guide to the Use of Statistical Methods in the Physical Sciences*. Wiley: Chichester, England.

Barry RG. 2008. *Mountain Weather and Climate*, 3rd edition. Cambridge University Press: Cambridge, England.

Beniston M, Diaz HF, Bradley RS. 1997. Climatic change at high elevation sites: an overview. *Climatic Change* **36**: 233–251. DOI:10.1023/A:1005380714349.

Berg NH. 1986. Blowing snow at a Colorado alpine site – measurements and implications. *Arctic and Alpine Research* **18**(2): 147–161. DOI:10.2307/1551124.

Berghuijs WR, Woods RA, Hrachowitz M. 2014. A precipitation shift from snow towards rain leads to a decrease in streamflow. *Nature Climate Change* **4**: 583–586. DOI:10.1038/NCLIMATE2246.

Black TA, DenHartog G, Neumann HH, Blanken PD, Yang PC, Russell C, Nesic Z, Lee X, Chen SG, Staebler R, Novak MD. 1996. Annual cycles of water vapour and carbon dioxide fluxes in and above a boreal aspen forest. *Global Change Biology* **2**(3): 219–229. DOI:10.1111/j.1365-2486.1996.tb00074.x.

Blanken PD, Willliams MW, Burns SP, Monson RK, Knowles J, Chowanski K, Ackerman T. 2009. A comparison of water and carbon dioxide exchange at a windy alpine tundra and subalpine forest site near Niwot Ridge, Colorado. *Biogeochemistry* **95**: 61–76. DOI:10.1007/s10533-009-9325-9.

Blonquist JM, Tanner BD, Bugbee B. 2009. Evaluation of measurement accuracy and comparison of two new and three traditional net radiometers. *Agricultural and Forest Meteorology* **149**: 1709–1721. DOI:10.1016/j.agrformet.2009.05.015.

Budyko MI. 1974. *Climate and Life*. Academic Press: New York, NY; 508.

Burns SP, Molotch NP, Williams MW, Knowles JF, Seok B, Monson RK, Turnipseed AA, Blanken PD. 2014. Snow temperature changes within a seasonal snowpack and their relationship to turbulent fluxes of sensible and latent heat. *Journal of Hydrometeorology* **15**(1): 117–142. DOI:10.1175/JHM-D-13-026.1.

Chauvin GM, Flerchinger GN, Link TE, Marks D, Winstral AH, Seyfried MS. 2011. Long-term water balance and conceptual model of a semi-arid mountainous catchment. *Journal of Hydrology* **400**: 133–143. DOI:10.1016/j.jhydrol.2011.01.031.

Chen X, Alimohammadi N, Wang D. 2013. Modeling interannual variability of seasonal evaporation and storage change based on the extended Budyko framework. *Water Resources Research* **49**: 6067–6078. DOI:10.1002/wrcr.20493.

Clow DW. 2010. Changes in the timing of snowmelt and streamflow in Colorado: a response to recent warming. *Journal of Climate* **23**(9): 2293–2306. DOI:10.1175/2009JCLI2951.1.

Cowie RC. 2010. The hydrology of headwater catchments from the plains to the Continental Divide, Boulder Creek watershed, Colorado, MA Thesis, Geography, University of Colorado.

Creed IF, Spargo AT, Jones JA, Buttle JM, Adams MB, Beall FD, Booth E, Campbell J, Clow D, Elder K, Green MB, Grimm NB, Miniat C, Ramlal P, Saha A, Sebestyen S, Spittlehouse D, Sterling S, Williams MW, Winkler R, Yao H. 2014. Changing forest water yields in response to climate warming: results from long-term experimental watershed sites across North America. *Global Change Biology* **20**: 3191–3208. DOI:10.1111/gcb.12615.

Creutzfeldt B, Troch PA, Güntner A, Ferré TPA, Graeff T, Merz B. 2014. Storage-discharge relationships at different catchment scales based on local high-precision gravimetry. *Hydrological Processes* **28**: 1465–1475. DOI:10.1002/hyp.9689.

Darrouzet-Nardi A, Erbland J, Bowman WD, Savarino J, Williams MW. 2012. Landscape-level nitrogen import and export in an ecosystem with complex terrain, Colorado Front Range. *Biogeochemistry* **109**(1–3): 271–285. DOI:10.1007/s10533-011-9625-8.

Dingman SL. 2002. *Physical Hydrology*, 2nd edition. Prentice Hall: Upper Saddle River, New Jersey; 646.

Donohue RJ, McVicar TR, Roderick ML. 2010. Assessing the ability of potential evaporation formulations to capture the dynamics in evaporative demand within a changing climate. *Journal of Hydrology* **386**: 186–197. DOI:10.1016/j.jhydrol.2010.03.020.

Elliott G. 2011. Influences of 20th-century warming at the upper tree line contingent on local-scale interactions: evidence from a latitudinal

gradient in the Rocky Mountains, USA. *Global Ecology and Biogeography* **20**: 46–57. DOI:10.1111/j.1466-8238.2010.00588.x.

Erickson TA, Williams MW, Winstral A. 2005. Persistence of topographic controls on the spatial distribution of snow in rugged mountain terrain, Colorado, United States. *Water Resources Research* **41**: W04014. DOI:10.1029/2003WR002973.

Fisher JB, Whittaker RJ, Malhi Y. 2010. ET come home: potential evapotranspiration in geographical ecology. *Global Ecology and Biogeography* **20**: 1–18. DOI:10.1111/j.1466-8238.2010.00578.x.

Flerchinger GN, Cooley KR. 2000. A ten-year water balance of a mountainous, semi-arid watershed. *Journal of Hydrology* **237**: 86–99. DOI:10.1016/S0022-1694(00)00299-7.

Foken T, Aubinet M, Leuning R. 2012. The eddy covariance method. In *Eddy Covariance: A Practical Guide to Measurement and Data Analysis*, Aubinet M, Vesala T, Papale D (eds). Springer Atmospheric Sciences: New York; 1–20.

French AN, Schmugge TJ, Kustas WP, Brubaker KL, Prueger J. 2003. Surface energy fluxes over El Reno, Oklahoma, using high-resolution remotely sensed data. *Water Resources Research* **39**(6): 1164. DOI:10.1029/2002WR001734.

Gable DJ, Madole RF. 1976. Geologic map of the Ward quadrangle, Boulder County, CO. U.S. Geological Survey Geologic Quadrangle Map GQ-1277.

Goulden ML, Anderson RG, Bales RC, Kelly AE, Meadows M, Winston GC. 2012. Evapotranspiration along an elevation gradient in California's Sierra Nevada. *Journal of Geophysical Research, Biogeosciences* **117**: G03028. DOI:10.1029/2012JG002027.

Graham CB, Verseveld WV, Barnard HR, McDonnell JJ. 2010. Estimating the deep seepage component of the hillslope and catchment water balance within a measurement uncertainty framework. *Hydrological Processes* **24**: 3631–3647. DOI:10.1002/hyp.7788.

Greenland D. 1989. The climate of Niwot Ridge, Front Range, Colorado, USA. *Arctic and Alpine Research* **21**(4): 380–391. DOI:10.2307/1551647.

Greenland D, Losleben MV. 2001. Climate. In *Structure and Function of an Alpine Ecosystem: Niwot Ridge, Colorado*, Bowman WD, Seastedt TR (eds). Oxford University Press: New York; 15–31.

Gu S, Tang YH, Cui XY, Du M, Zhao L, Li Y, Xu SX, Zhou H, Kato T, Qi PT, Zhao X. 2008. Characterizing evaporation over a meadow ecosystem on the Qinghai-Tibetan plateau. *Journal of Geophysical Research, [Atmospheres]* **113**: D08118. DOI:10.1029/2007JD009173.

Gutmann ED, Rasmussen RM, Liu CH, Ikeda K, Gochis DJ, Clark MP, Dudhia J, Thompson G. 2012. A comparison of statistical and dynamical downscaling of winter precipitation over complex terrain. *Journal of Climate* **25**(1): 262–281. DOI:10.1175/2011JCLI4109.1.

Hamon WR. 1963. Computation of direct runoff amounts from storm rainfall. *International Association of Scientific Hydrology. Publication* **63**: 52–62.

Harpold AA, Brooks PD, Rajogopalan S, Heidebuchel I, Jardine A, Stielstra C. 2012. Changes in snowpack volume and snowmelt timing in the Intermountain West. *Water Resources Research* **48**: W11501. DOI:10.1029/2012WR011949.

Hollinger DY, Aber J, Dail B, Davidson EA, Goltz SM, Hughes H, Leclerc MY, Lee JT, Richardson AD, Rodrigues C, Scott NA, Achuatavarier D, Walsh J. 2004. Spatial and temporal variability in forest-atmosphere CO_2 exchange. *Global Change Biology* **10**: 1689–1706. DOI:10.1111/j.1365-2486.2004.00847.x.

Hong SH, Hendrickx JMH, Borchers B. 2009. Up-scaling of SEBAL derived evapotranspiration maps from Landsat (30 m) to MODIS (250 m) scale. *Journal of Hydrology* **370**: 122–138. DOI:10.1016/j.jhydrol.2009.03.002.

Hood E, Williams MW, Cline D. 1999. Sublimation from a seasonal snowpack as a continental, mid-latitude alpine site. *Hydrological Processes* **13**: 1781–1797.

Janowicz JR, Hedstrom N, Pomeroy J, Granger R, Carey S. 2004. Wolf Creek Research Basin water balance studies. Northern Research Basins Water Balance (Proceedings of a workshop held at Victoria, Canada, March 2004). IAHS Publ. 290; 195–204.

Jenks GF. 1967. The data model concept in statistical mapping. *International Yearbook of Cartography* **7**: 186–190.

Jones JA, Creed IF, Hatcher KL, Warren RJ, Adams M, Benson MH, Boose E, Brown WA, Campbell JL, Covich A, Clow DW, Dahm CN, Elder K, Ford CR, Grimm NB, Henshaw DL, Larson KL, Miles ES, Miles KM, Sebestyen SD, Spargo AT, Stone AB, Vose JM, Williams MW. 2012. Ecosystem processes and human influences regulate streamflow response to climate change at long term ecological research sites. *BioScience* **62**(4): 390–404. DOI:10.1525/bio.2012.62.4.10.

Kane DL, Yang D (eds). 2004. Northern Research Basins Water Balance. IAHS Series of Proceedings and Reports: Publication 290. Oxford, UK; 271 pp.

Kattelmann R, Elder K. 1991. Hydrologic characteristics and water balance of an alpine basin in the Sierra Nevada. *Water Resources Research* **27**(7): 1553–1562. DOI:10.1029/90WR02771.

Knowles N, Dettinger MD, Cayan DR. 2006. Trends in snowfall versus rainfall in the Western United States. *Journal of Climate* **19**(18): 4545–4559. DOI:10.1175/JCLI3850.1.

Knowles JF, Blanken PD, Williams MW, Chowanski KM. 2012. Energy and surface moisture seasonally limit evaporation and sublimation from snow-free alpine tundra. *Agricultural and Forest Meteorology* **157**: 106–115. DOI:10.1016/j.agrformet.2012.01.017.

Knowles JF, Burns SP, Blanken PD, Monson RK. 2014. Fluxes of energy, water, and carbon dioxide from mountain ecosystems at Niwot Ridge, Colorado. *Plant Ecology and Diversity* . DOI:10.1080/17550874.2014.904950.

Lee X, Massman W, Law B. 2004. *Handbook of Micrometeorology: A Guide for Surface Flux Measurements and Analysis*. Kluwer Academic Publishers: Dordrecht, Netherlands; 250.

Lewis WM, Grant MC. 1979. Changes in the output of ions from a watershed as a result of the acidification of precipitation. *Ecology* **60**: 1093–1097.

Lu J, Sun G, McNulty SG, Amatya DM. 2005. A comparison of six potential evapotranspiration methods for regional use in the southeastern United States. *Journal of the American Water Resources Association* **41** (3): 621–633. DOI:10.1111/j.1752-1688.2005.tb03759.x.

MacDonald MK, Pomeroy JW, Pietroniro A. 2010. On the importance of sublimation to an alpine snow mass balance in the Canadian Rocky Mountains. *Hydrology and Earth System Sciences* **14**: 1401–1415. DOI:10.5194/hess-14-1401-2010.

Mackun P, Wilson S. 2011. Population distribution and change: 2000 to 2010. 2010 Census Briefs, United States Census 2010, US Census Bureau, Report Number C2010BR-01.

McAfee SA. 2013. Methodological differences in projected potential evapotranspiration. *Climatic Change* **120**: 915–930. DOI:10.1007/s10584-013-0864-7.

Molotch NP, Blanken PD, Williams MW, Turnipseed AA, Monson RK, Margulis S. 2007. Estimating sublimation of intercepted and sub-canopy snow using eddy covariance systems. *Hydrological Processes* **21**(12): 1567–1575. DOI:10.1002/hyp.6719.

Moncrieff JB, Malhi Y, Leuning R. 1996. The propagation of errors in long-term measurements of land-atmosphere fluxes of carbon and water. *Global Change Biology* **2**: 231–240. DOI:10.1111/j.1365-2486.1996.tb00075.x.

Moore DJP, Hu J, Sacks WJ, Schimel DS, Monson RK. 2008. Estimating transpiration and the sensitivity of carbon uptake to water availability in a subalpine forest using a simple ecosystem process model informed by measured net CO_2 and H_2O fluxes. *Agricultural and Forest Meteorology* **148**: 1467–1477. DOI:10.1016/j.agrformet.2008.04.013.

Murphy SF, Verplanck PL, Barber LB (eds). 2003. Comprehensive water quality of the Boulder Creek watershed, Colorado, during high-flow and low-flow conditions, 2000. USGS Water-Resources Investigations Report 2003–4045, xiii; 198 pp.

Nayak A, Marks D, Chandler CG, Seyfried M. 2010. Long-term snow, climate, and streamflow trends at the Reynolds Creek Experimental Watershed, Owyhee Mountains, Idaho, United States. *Water Resources Research* **46**: W06519. DOI:10.1029/2008WR007525.

Peichl M, Sagerfors J, Lindroth A, Buffam I, Grelle A, Klemedtsson L, Laudon H, Nilsson MB. 2013. Energy exchange and water budget partitioning in a boreal minerogenic mire. *Journal of Geophysical Research, Biogeosciences* **118**: 1–13. DOI:10.1029/2012JG002073.

Penman HL. 1948. Natural evaporation from open water, bare soil and grass. *Proceedings of the Royal Society of London Series A-Mathematical and Physical Sciences* **193**(1032): 120–145. DOI:10.1098/rspa.1948.0037.

Priestley CHB, Taylor RJ. 1972. On the assessment of surface heat flux and evaporation using large scale parameters. *Monthly Weather Review*

100: 81–92. DOI:10.1175/1520-0493(1972)100<0081:OTAOSH>2.3.CO;2.

Rasmussen R, Liu CH, Ikeda K, Gochis D, Yates D, Chen F, Tewari M, Barlage M, Dudhia J, Yu W, Miller K, Arsenault K, Grubisic V, Thompson G, Gutmann E. 2011. High-resolution coupled climate runoff simulations of seasonal snowfall over Colorado: a process study of current and warmer climate. *Journal of Climate* **24**(12): 3015–3048. DOI:10.1175/2010JCLI3985.1.

Rasmussen R, Baker B, Kochendorfer J, Meyers T, Landolt S, Fischer AP, Black J, Thériault JM, Kucera P, Gochis D, Smith C, Nitu R, Hall M, Ikeda K, Gutmann E. 2012. How well are we measuring snow? The NOAA/FAA/NCAR winter precipitation test bed. *Bulletin of the American Meteorological Society* **93**(6): 811–829. DOI:10.1175/BAMS-D-11-00052.1.

Roderick ML, Farquhar GD. 2011. A simple framework for relating variations in runoff to variations in climatic conditions and catchment properties. *Water Resources Research* **47**: W00G07. DOI:10.1029/2010WR009826.

Seastedt TR, Bowman WD, Caine TN, McKnight D, Townsend A, Williams MW. 2004. The landscape continuum: a model for high-elevation ecosystems. *BioScience* **54**(2): 111–121. DOI:10.1641/0006-3568(2004)054[0111:TLCAMF]2.0.CO;2.

Segura C, Pitlick J. 2010. Scaling frequency of channel-forming flows in snowmelt-dominated streams. *Water Resources Research* **46**: W06524. DOI:10.1029/2009WR008336.

Serreze MC, Clark MP, Armstrong RL, McGinnis DA, Pulwarty RS. 1999. Characteristics of the Western United States snowpack from snowpack telemetry (SNOTEL) data. *Water Resources Research* **35**: 2145–2160. DOI:10.1029/1999WR900090.

Shuttleworth JW. 1993. Evaporation. In *Handbook of Hydrology*, Maidment DR (ed). McGraw-Hill: New York, NY; 4.1–4.53.

Stednick JD. 1981. Hydrochemical balance of an alpine watershed in Southeast Alaska. *Arctic and Alpine Research* **13**(4): 431–438. DOI:10.2307/1551054.

Stewart IT, Cayan DR, Dettinger MD. 2004. Changes in snowmelt runoff timing in Western North America under a 'business as usual' climate change scenario. *Climatic Change* **62**: 217–232. DOI:10.1023/B:CLIM.0000013702.22656.e8.

Stewart IT, Cayan DR, Dettinger MD. 2005. Changes toward earlier streamflow timing across Western North America. *Journal of Climate* **18**: 1136–1155. DOI:10.1175/JCLI3321.1.

Strasser U, Bernhardt M, Weber M, Liston GE, Mauser W. 2008. Is snow sublimation important to the alpine water balance? *The Cryosphere* **2** (1): 53–66.

Tabler RD. 2003. Controlling blowing and drifting snow with snow fences and road design. National Cooperative Highway Research Program Transportation Research Board of the National Academies; 307 pp.

Tague C, Peng H. 2013. The sensitivity of forest water use to the timing of precipitation and snowmelt recharge in the California Sierra: implications for a warming climate. *Journal of Geophysical Research, Biogeosciences* **118**: 875–887. DOI:10.1002/jgrg.20073.

Tague C, Heyn K, Christensen L. 2009. Topographic controls on spatial patterns of conifer transpiration and net primary productivity under climate warming in mountain ecosystems. *Ecohydrology* **2**: 541–554. DOI:10.1002/eco.88.

Taylor JR. 1997. *An Introduction to Error Analysis*. University Science Books: Sausalito, CA; 327.

Thornthwaite CW, Mather JR. 1957. Instructions and tables for computing potential evapotranspiration and the water balance. *Publications in Climatology*, Drexel Institute of Technology, Laboratory of Climatology: Centerton, NJ; **10**(3): 126.

Turnipseed AA, Blanken PD, Anderson DE, Monson RK. 2002. Energy budget above a high-elevation subalpine forest in complex topography. *Agricultural and Forest Meteorology* **110**(3): 177–201. DOI:10.1016/S0168-1923(01)00290-8.

Vasilenko NG. 2004. Water balance of small Russian catchments in the southern mountainous Taiga Zone: "Mogot" case study. Northern Research Basins Water Balance (Proceedings of a workshop held at Victoria, Canada, March 2004). IAHS Publ. 290; 65–77.

Vörösmarty CJ, Green P, Salisbury J, Lammers RB. 2000. Global water resources: vulnerability from climate change and population growth. *Science* **289**(5477): 284–288. DOI:10.1126/science.289.5477.284.

Walker MD, Walker DA, Theodose TA, Webber PJ. 2001. The vegetation: hierarchical species-environment relationships. In *Structure and Function of an Alpine Ecosystem: Niwot Ridge, Colorado*, Bowman WD, Seastedt TR (eds). Oxford University Press: New York; 99–127.

Wetherbee GA, Rhodes MF, Ludtke A. 2013. Statistical comparison of OTT Pluvio-2 and Belfort 5–780 weekly precipitation records. Abstract: National Atmospheric Deposition Program Annual Meeting: Park City, UT, 8–11 October 2013.

Williams MW, Losleben M, Caine N, Greenland D. 1996. Changes in climate and hydrochemical responses in a high-elevation catchment in the Rocky Mountains, USA. *Limnology and Oceanography* **41**(5): 939–946.

Williams MW, Bardsley T, Rikkers M. 1998. Overestimation of snow depth and inorganic nitrogen wetfall using NADP data, Niwot Ridge, Colorado. *Atmospheric Environment* **32**(22): 3827–3833. DOI:10.1016/S1352-2310(98)00009-0.

Williams MW, Cline D, Hartmann M, Bardsley T. 1999. Data for snowmelt model development, calibration, and verification at an alpine site, Colorado Front Range. *Water Resources Research* **35**(10): 3205–3209. DOI:10.1029/1999WR900088.

Williams MW, Barnes TR, Parman JN, Freppaz M, Hood E. 2011. Stream water chemistry along an elevational gradient from the Continental Divide to the foothills of the Rocky Mountains. *Vadose Zone Journal* **10**: 900–914. DOI:10.2136/vzj2010.0131.

Williams CA, Reichstein M, Buchmann N, Baldocchi D, Beer C, Schwalm C, Wohlfahrt G, Hasler N, Bernhofer C, Foken T, Papale D, Schymanski S, Schaefer K. 2012. Climate and vegetation controls on the surface water balance: synthesis of evapotranspiration measured across a global network of flux towers. *Water Resources Research* **48**: W06523. DOI:10.1029/2011WR011586.

Yao H. 2009. Long-term study of lake evaporation and evaluation of seven estimation methods: results from Dickie Lake, South-central Ontario, Canada. *Journal of Water Resource and Protection* **2**: 59–77. DOI:10.4236/jwarp.2009.12010.

Yao H, Creed IF. 2005. Determining spatially-distributed annual water balances for ungauged locations on Shikoku Island, Japan: a comparison of two interpolators. *Hydrological Sciences Journal* **50**: 245–263. DOI:10.1623/hysj.50.2.245.61792.

Zhuravin SA. 2004. Features of water balance for small mountainous watersheds in East Siberia: Kolyma Water Balance Station case study. Northern Research Basins Water Balance (Proceedings of a workshop held at Victoria, Canada, March 2004). IAHS Publ. 290; 28–40.

